Supplementary

Effect of fluorinated arylammonium halides passivation in chloride-iodide perovskite solar cell

Ashraful Hossain Howlader[1]*, Yao Yin[2], Rhiannon Kuchel[2], and Ashraf Uddin[1]*

[1]School of Photovoltaic and Renewable Energy Engineering, UNSW Sydney, NSW 2052, Australia

[2]Mark Wainwright Analytical Centre, UNSW Sydney, NSW 2052, Australia

*Email: a.howlader@unsw.edu.au, a.uddin@unsw.edu.au

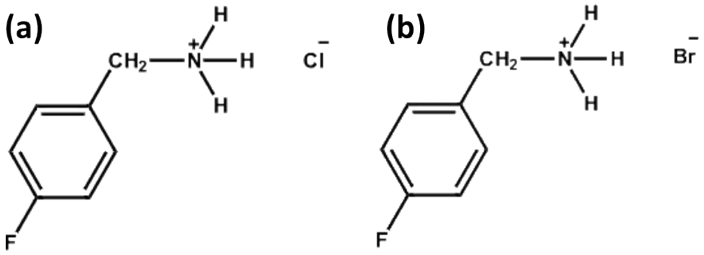

Figure S1: Chemical structures of **(a)** 4-FBAC, **(b)** 4-FBAB. The images are taken from www.greatcellsolarmaterials.com on 1st October 2025.

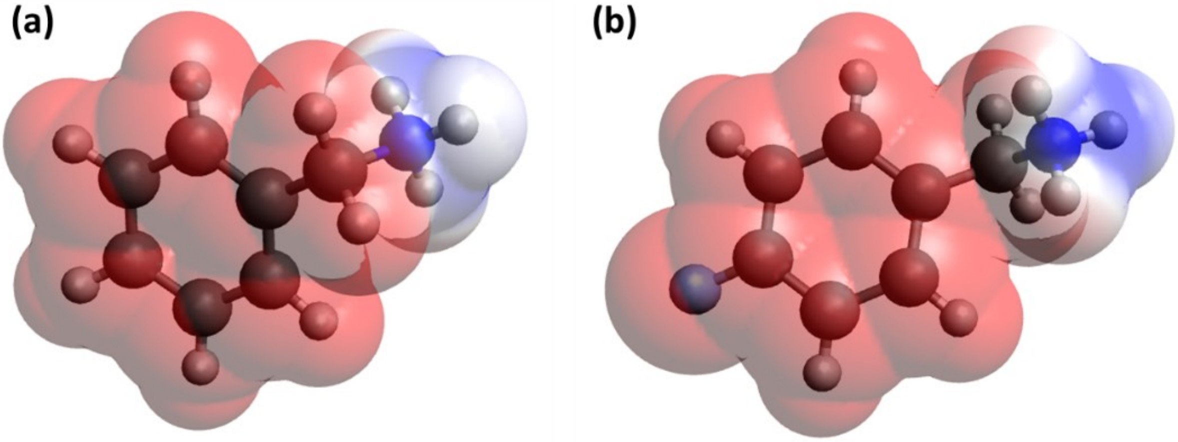

Figure S2: ESP maps of **(a)** BA and **(b)** 4-FBA. The red colour is for positive potential and the blue color is for the negative potential.

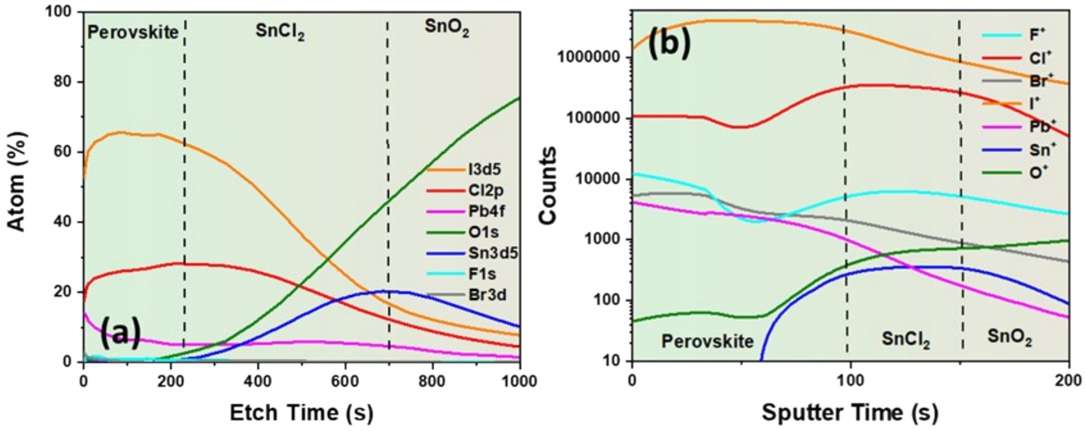

Figure S3: Depth-dependent **(a)** XPS and **(b)** TOF-SIMS from the buried interface of the passivated chloride-iodide perovskite sample. Both figures are divided into three regions with the black dotted lines. The left (the top side) region is the perovskite layer, the middle region is the self-formed $SnCl_2$ layer, and the right (the bottom side) region is the SnO_2 layer.

Table S1: Halogen atom percentage variation in the bulk of passivated chloride-iodide perovskite thin film from EDS. With an increasing angle, the analysis depth increases.

Element/Angle	**30°**	**45°**	**60°**	**90°**
F (%)	3.90	2.60	1.80	1.60
Cl (%)	2.60	3.10	3	2.50
Br (%)	28.60	29.40	32.80	37.30
I (%)	65	65	62.30	58.60

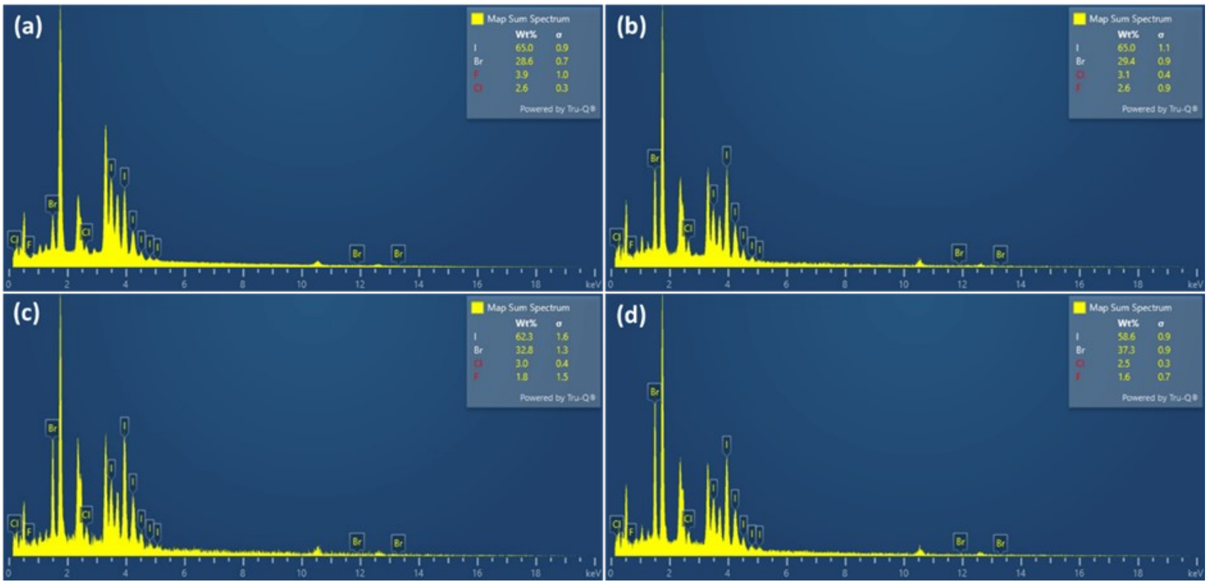

Figure S4: Halide ions percentage variation in the bulk of passivated chloride-iodide perovskite thin film from EDS. With an increasing angle, the analysis depth increases. The angle between the film surface and the electron beam is **(a)** 30°, **(b)** 45°, **(c)** 60°, and **(d)** 90°.

Table S2: Atomic percentages of different elements taken from XPS on the surface of non-passivated and passivated chloride-iodide perovskite samples.

	C (%)	N (%)	Pb (%)	F (%)	Cl (%)	Br (%)	I (%)
Non-passivated	18.39	20.47	11.76	0	5.88	0	42.49
Passivated	39.51	12.53	8.17	4.31	7.28	1.00	24.82

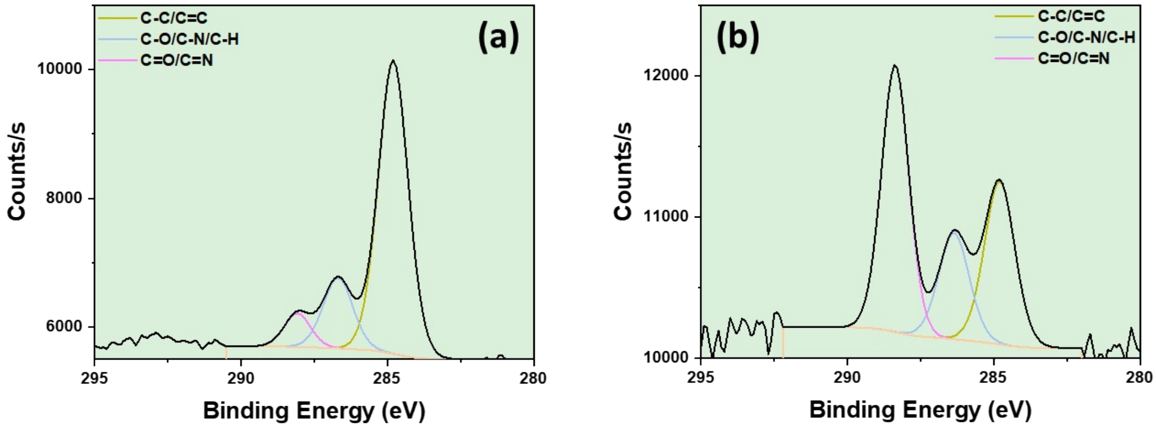

Figure S5: XPS analysis from the top surface of the **(a)** non-passivated and **(b)** passivated chloride-iodide perovskite samples.

Table S3: Comparison of the intensity of different C bonds originating from C1s of non-passivated and passivated chloride-iodide perovskite samples from XPS.

	C-C/C=C (284.8 eV)	C-O/C-N/C-H (286.6 eV)	C=O/C=N (288.6 eV)
Non-passivated	10121	6770	6195
Passivated	11241	10882	12065

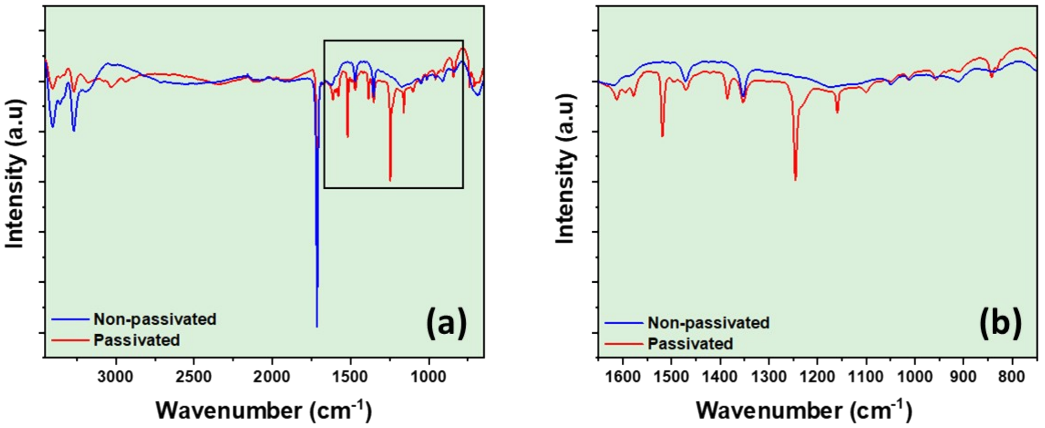

Figure S6. (a) FTIR analysis from the top surface of both chloride-iodide perovskite samples (non-passivated and passivated). In the inset, the peaks corresponding to the range 800-1600 cm^{-1} are shown, which is represented in **(b)**.

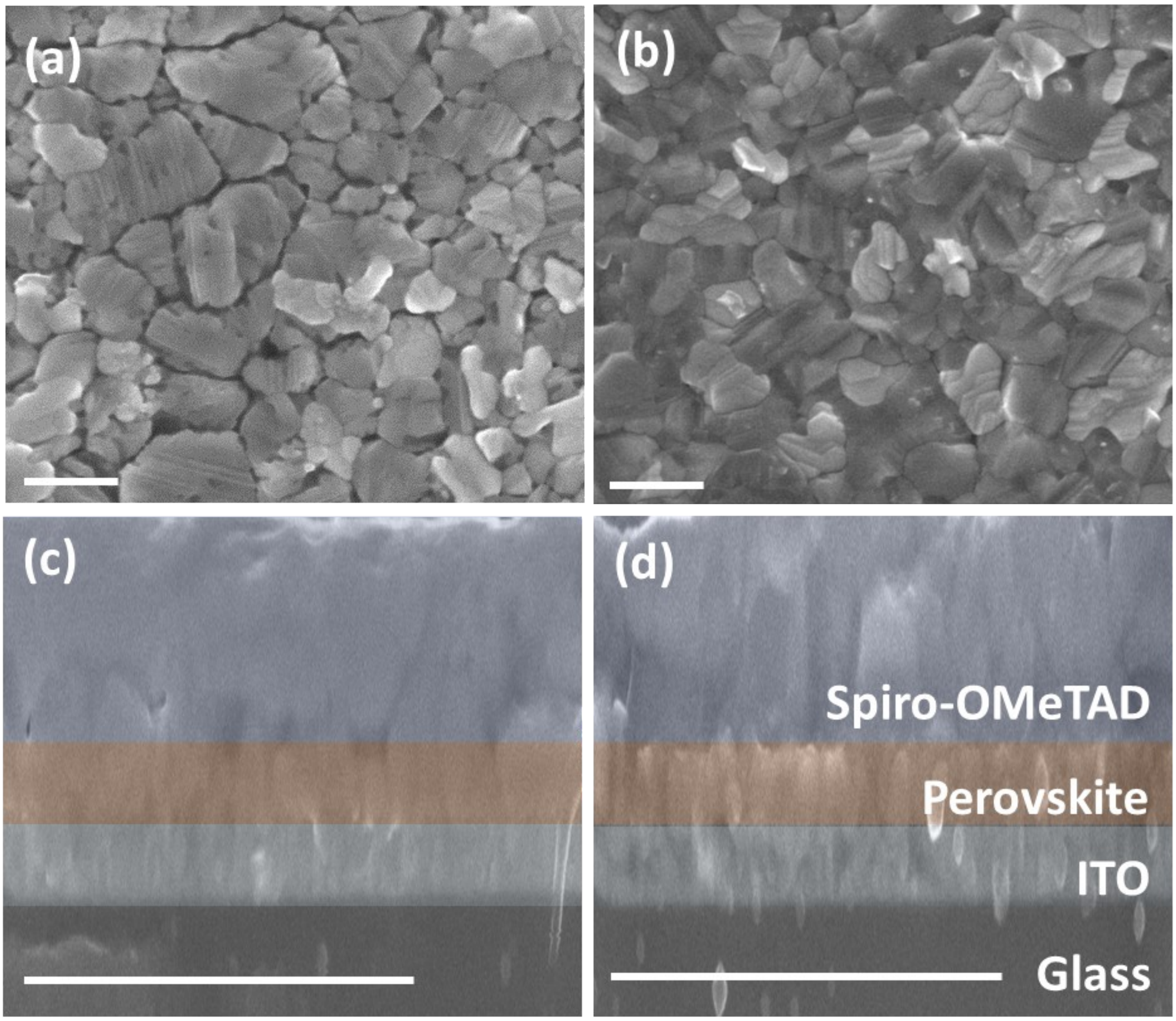

Figure S7: SEM images of **(a)** non-passivated and **(b)** passivated chloride-iodide perovskite samples. The SEM images are taken from the top surface of the chloride-iodide perovskite samples. Cross-sectional images of **(b)** non-passivated and **(d)** passivated chloride-iodide perovskite samples. Different layers in the cross-sections are indicated with other colors. The scale bars in all the figures are 500 nm.

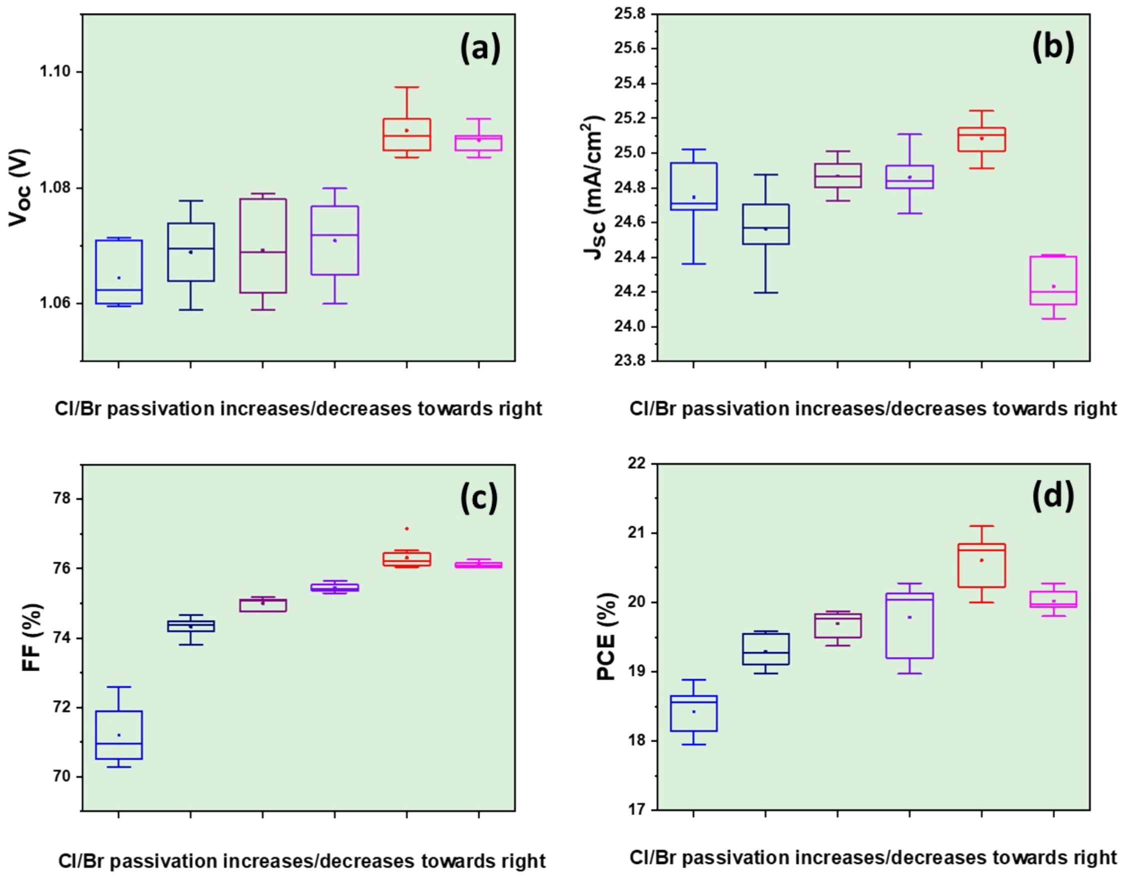

Figure S8: Statistical variation of key photovoltaic parameters of non-passivated and passivated cells with Cl and Br ratio variation (here, 6 cells of each type are used): **(a)** V_{oc}, **(b)** J_{sc}, **(c)** FF, **(d)** PCE. The Cl passivation increases toward the right, while the Br passivation increases toward the left. Each step value is 25%. The first one from the left is the non-pasivated control cell.

Table S4: The average with standard deviation values and the champion values of each key photovoltaic parameter (V_{oc}, J_{sc}, FF, and PCE) for 6 samples of each type of chloride-iodide PSC: without passivation and with passivation (variation of Cl and Br percentages).

		V_{oc} (V)	J_{sc} (mA/cm^2)	FF (%)	PCE (%)
0% F & 0% Cl & 0% Br (Non-passivated PSC)	**Average**	1.06±0.01	24.74±0.20	71.20±0.84	18.42±0.32
	Champion	1.07	24.73	71.28	18.90
100% F & 0% Cl & 100% Br (Passivated PSC)	**Average**	1.06±0.01	24.56±0.23	74.32±0.30	19.30±0.24
	Champion	1.07	24.70	74.20	19.60
100% F & 25% Cl & 75% Br (Passivated PSC)	**Average**	1.07±0.01	24.86±0.11	75±0.18	19.70±0.20
	Champion	1.07	24.73	75.19	19.87
100% F & 50% Cl & 50% Br (Passivated PSC)	**Average**	1.07±0.01	24.86±0.16	75.45±0.13	19.80±0.51
	Champion	1.08	24.33	75.40	20.30
100% F & 75% Cl & 25% Br (Passivated PSC) (Champion PSC)	**Average**	1.09±0.01	25.08±0.10	76.32±0.32	20.64±0.40
	Champion	1.10	25.15	76.44	21.10
100% F & 100% Cl & 0% Br (Passivated PSC)	**Average**	1.09±0.00	24.23±0.55	76.15±0.83	20.02±0.17
	Champion	1.09	23.60	76.05	20.27

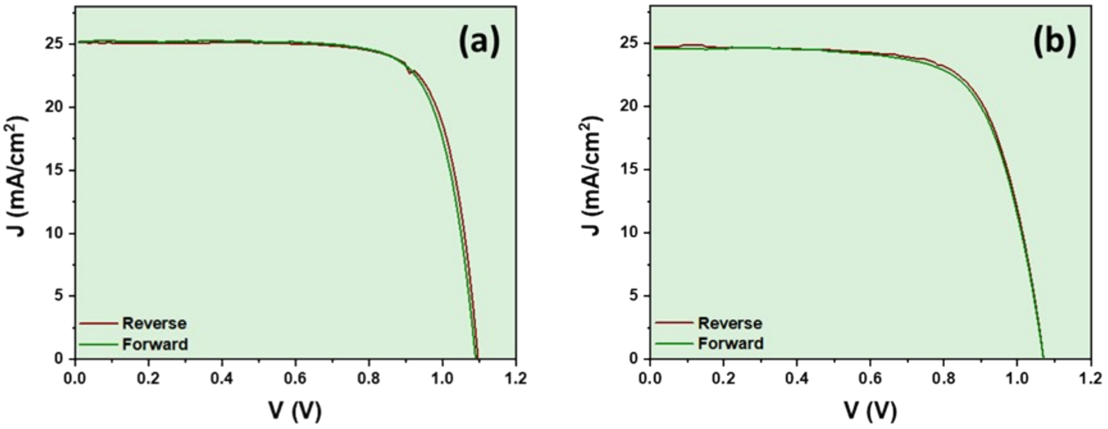

Figure S9: Forward and reverse J-V curves of **(a)** non-passivated control and **(b)** passivated champion chloride-iodide PSCs.

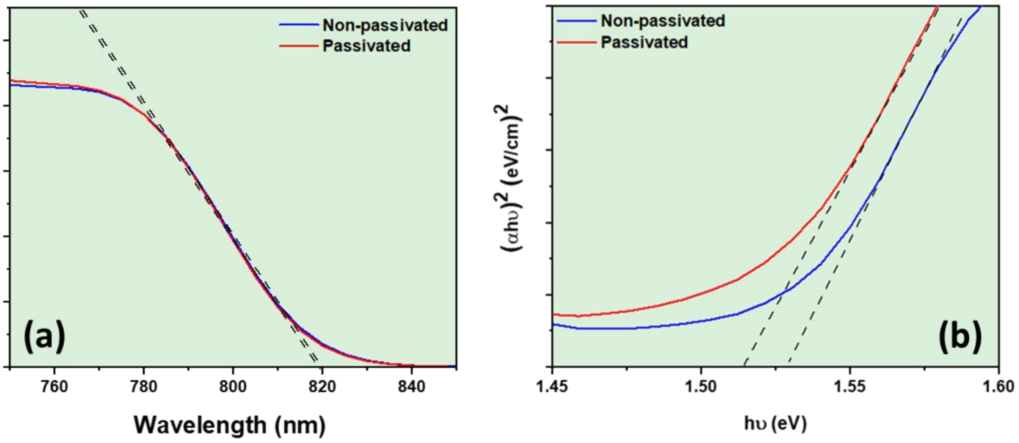

Figure S10: **(a)** Cut-off wavelengths of both PSCs (non-passivated control and passivated champion) and **(b)** Tauc's plot of both samples (non-passivated control and passivated champion).

Table S5: The TRPL curves of the two samples (non-passivated control and passivated champion) are fitted with an exponential second-order decay equation of $y = A_1 e^{t_1} + A_2 e^{t_2}$, where A_1 and A_2 are coefficients and t_1 and t_2 are time constants.

	A_1	**t_1 (ns)**	**A_2**	**t_2 (ns)**
0% F & 0% Cl & 0% Br	17.09	4.41	0.35	39.38
100% F & 75% Cl & 25% Br	5.80	6.27	0.35	51.70

Table S6: Resistance and capacitance values of series resistance (R_S), high-frequency resistance (R_H), high-frequency capacitance (C_H), low-frequency resistance (R_L), and low-frequency resistance (C_L) of two PSCs (non-passivated control and passivated champion cells).

	R_S	**R_H**	**C_H**	**R_L**	**C_L**
0% F & 0% Cl & 0% Br	613 Ω	371 kΩ	1.08 nF	7.29 MΩ	42.7 nF
100% F & 75% Cl & 25% Br	567 Ω	349 kΩ	1.09 nF	5.15 MΩ	47.2 nF